MICRO-TSUNAMI DETECTED BY A REAL-TIME CABLE SYSTEM*

Hiroyuki Matsumoto and Kenji Hirata

Deep Sea Research Department, Japan Marine Science and Technology Center
2-15, Natsushima-cho, Yokasuka 237-0061, Japan
E-mail: **hmatsumoto@jamstec.go.jp**

1. INTRODUCTION

In order to monitor seismic activities and tsunami signals offshore, Japan Marine Science and Technology Center (JAMSTEC) in 1999 developed the second cable seafloor observatory in the Southern Kuril subduction zone off Hokkaido Island, Japan [Hirata *et al.*, 2002]. The observatory consists of three ocean-bottom seismographs (OBSs) and two ocean-bottom pressure gauges (PGs). All the observed data from these ocean-bottom sensors are transmitted through an optical cable to the coast stations including the headquarters of the JAMSTEC (Figure 1).

A moderate-to-large earthquake ($M_w = 6.8$) occurred at 14:21 GMT on 28 January, 2000 eastward from Hokkaido Island, Japan (Figure 1). Our cable seafloor observatory detected a micro-tsunami generated by the earthquake, though any conventional coastal tide gauges located nearby could not because of too small wave amplitude in comparison with background noise.

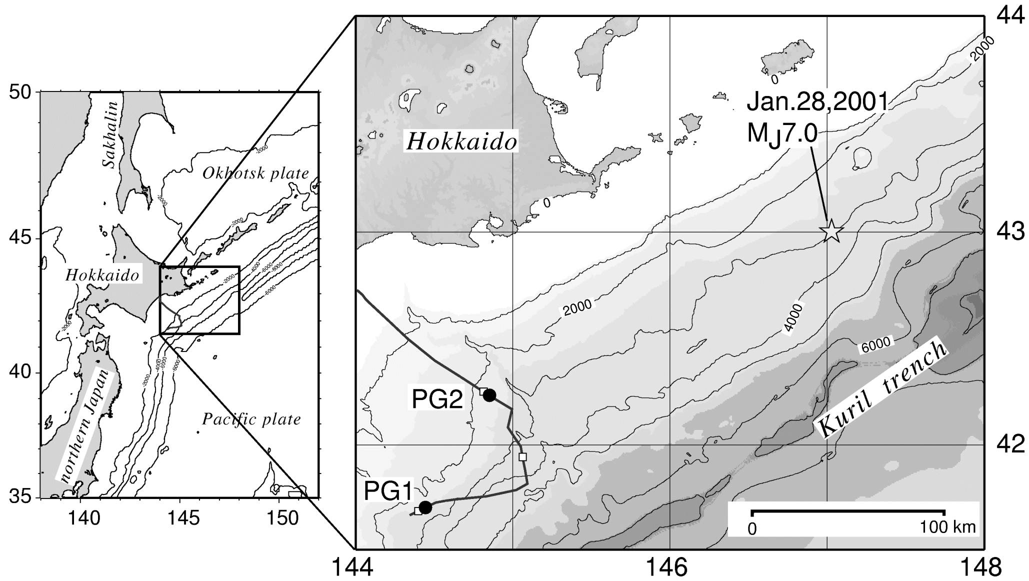

Figure 1. Location map for the epicenter (star) of the 28 January, 2000 earthquake and two ocean-bottom pressure gauges (solid circle) south of Hokkaido, Japan. A line connecting the ocean-bottom sensors offshore indicates the cable of the seep seafloor observatory of JAMSTEC. M_j is the JMA magnitude scale.

* Edited by A. B. Rabinovich

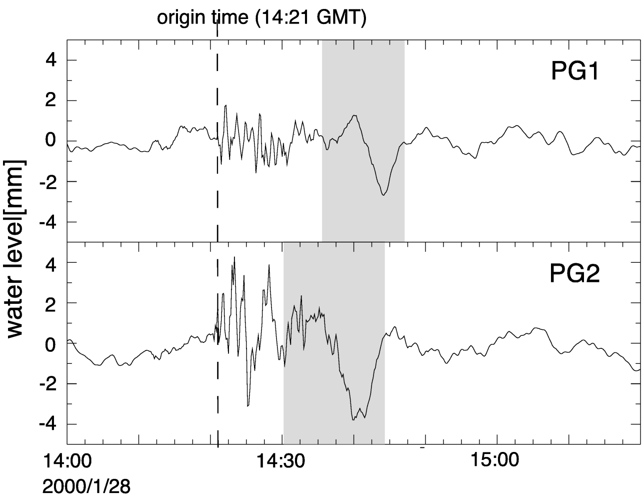

Figure2. The micro-tsunami generated by the 2000 event observed by two ocean-bottom pressure gauges offshore from Hokkaido Island. A dashed vertical line denotes the origin time of the earthquake. Signal of the micro-tsunami is hatched.

In the present study, we try to simulate this micro-tsunami by using numerical computation that considers dynamic contribution of the fault rupturing.

2. MICRO-TSUNAMI DETECTED BY PGS

Two PGs, PG1 and PG2, were deployed at depths of 2283 m and 2248 m, respectively. These locations are about 250 km and 190 km, respectively, from the epicenter of the earthquake (Figure 1). The micro-tsunami detected by the PGs is shown in Figure 2.

For both the PGs, the micro-tsunami began with a flood motion. Peak-to-trough wave heights of the observed micro-tsunamis are about 4 and 6 mm for PG1 and PG2, respectively.

3. ANALYTICAL PROCEDURE

In the present tsunami simulation technique, weak coupling is assumed between the seabed and seawater. That means that the motion of the seawater is influenced by the seabed motion, but the latter is not influenced by the former. Based on this assumption, seawater disturbances, including tsunamis, are simulated by providing the fluid domain at the seabed with the velocity of the seabed earthquake motion as an input function. Consequently, the present analysis consists of two-step simulation. The first step is to simulate the dynamic seabed displacement resulting from the seismic faulting, and the second is to simulate generation of the seawater disturbance followed by this displacement.

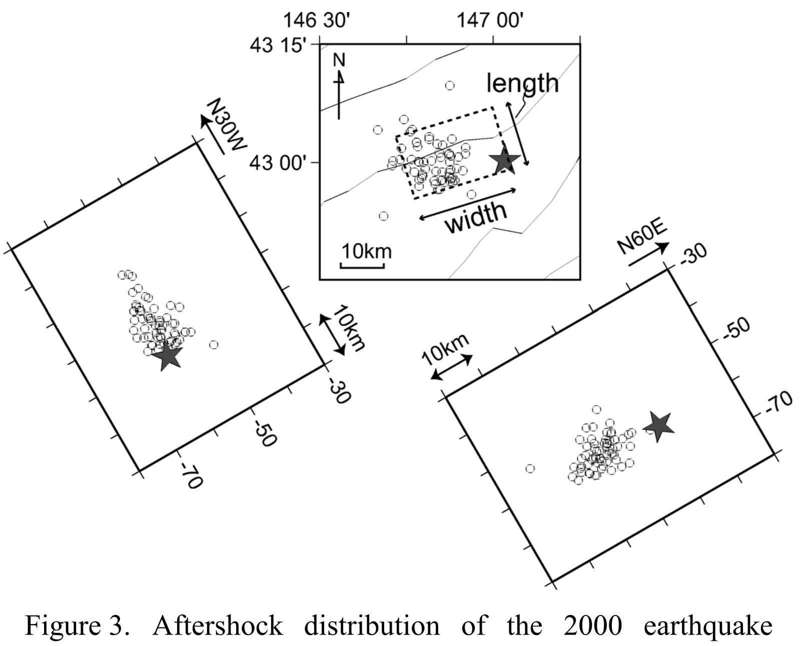

Figure 3. Aftershock distribution of the 2000 earthquake determined by Takahashi and Hirata (2002). Assumed fault plane is shown by the dashed line of (width 15 km and length 30 km).

For the first step simulation of the seabed displacement, the boundary element method (BEM) is employed here. The second step simulation of the seawater disturbances (i.e.

tsunami waves) is conducted by the finite difference method (FDM). The detailed formulations are described elsewhere [Ohmachi *et al.*, 2001].

Table 1

Fault parameters for the 28 January, 2000 earthquake (M_w = 6.8) occurred in the Southern Kuril subduction zone.

Width	30 km
Length	15 km
Focal depth	38 km
Dip	38 deg
Rake	195 deg
Dislocation	87 cm
Rupture velocity	3 km/sec
Rise time	2 sec

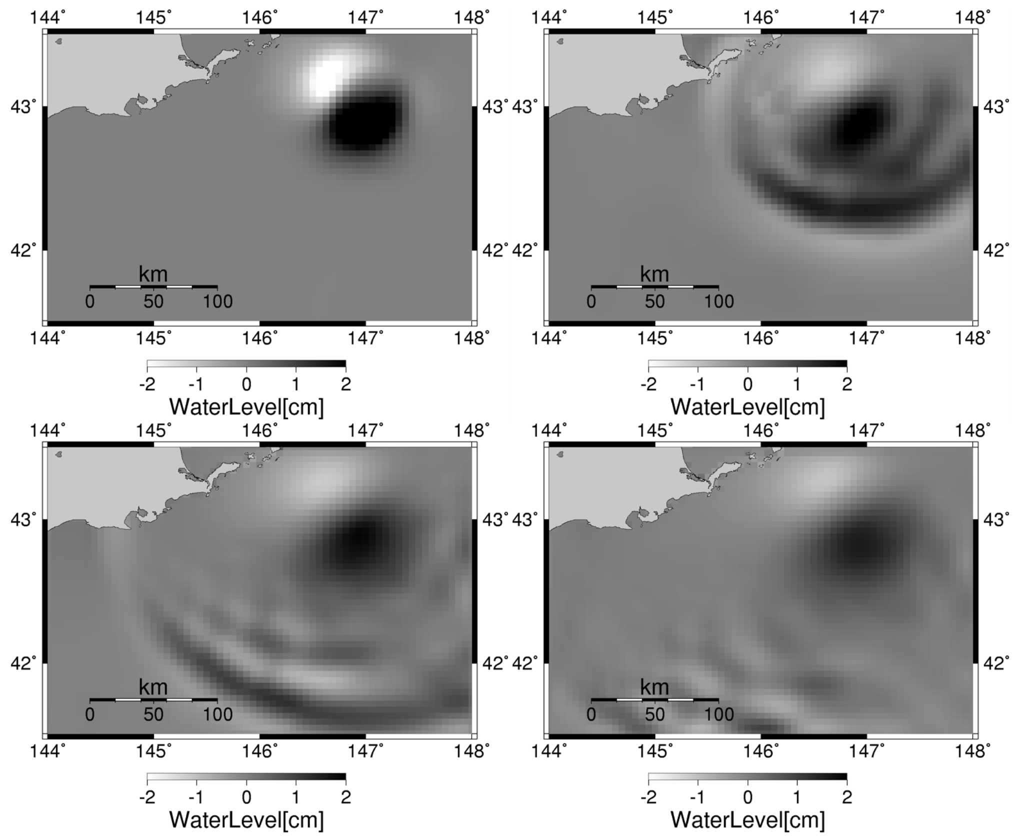

Figure 4. Simulated sea surface disturbance. Time = (a) 20 sec; (b) 40 sec; (c) 60 sec; (d) 80 sec.

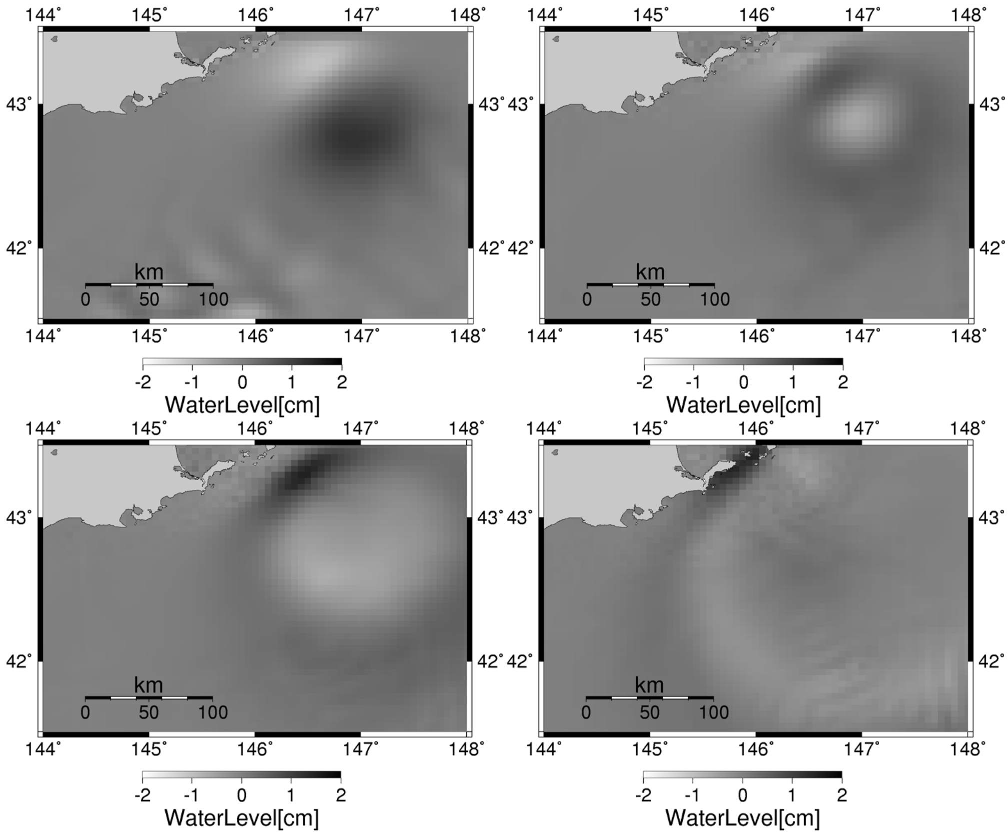

Figure 5. Simulated micro-tsunami propagation. Time = (a) 100 sec; (b) 200 sec; (c) 400 sec; (d) 800 sec.

4. NUMERICAL COMPUTATIONS OF THE MICRO-TSUNAMI

The micro-tsunami is simulated here using the 3-D modeling. In this study, we assume the Harvard CMT solution as the focal mechanism of the earthquake. Takahashi and Hirata [2002] examined aftershocks for a month after the earthquake using a modified master event method and suggested that the earthquake is an intra-slab event that ruptured on a shallow-dipping fault plane (Figure 3). They estimated the fault size of 30 km length and 15 km width for the earthquake. Therefore, for numerical computations we set a rectangular fault plane with the 30 km width and 15 km length. We also fix the strike, dip, and rake angles, describing the focal mechanism, based on the Harvard CMT solution. As a result, fault parameters shown in Table 1 are used in the following simulation.

Snapshots in Figure 4 show the sea surface disturbance resulting from the simulation at 20, 40, 60 and 80 sec after the fault rupturing. A disturbance propagating with faster velocity than a gravity water wave is associated with the Rayleigh wave propagating along the seabed. The water wave generated near the fault plane is the micro-tsunami caused by the static displacement of the seabed.

Snapshots in Figure 5 show the simulated micro-tsunami at 100, 200, 400, and 800 sec after the fault rupturing. The micro-tsunami propagates in accordance to the shallow water theory. This micro-tsunami passes over the PGs and its arrival times to the PG2 and PG1 sites are about 700 sec and 900 sec, respectively.

Time evolution tsunami records at PG1 and PG2 resulting from the simulation are compared with the observations (Figure 6). Each pair of the simulated and observed records corresponds well with respect to amplitude and arrival time of the major phase of the micro-tsunami. In addition, it should be noted that the short-period disturbance is seen in both the PGs and the simulation.

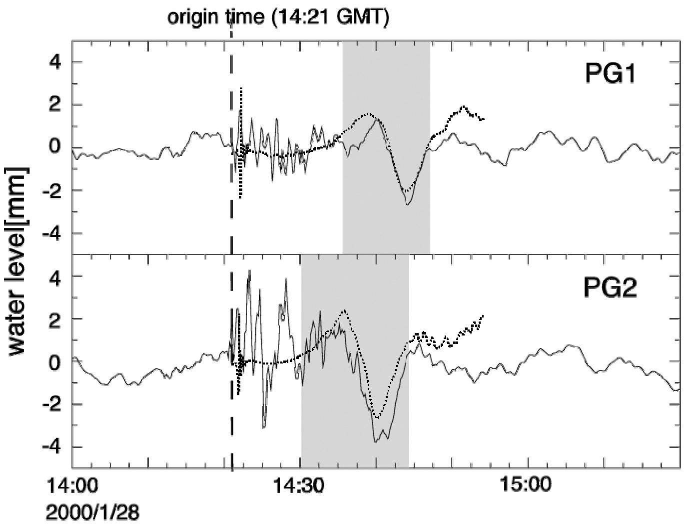

Figure 6. Comparison between observed (solid lines) and calculated (dashed lines) micro-tsunami for bottom pressure stations PG1 and PG2.

5. DISCUSSION AND CONCLUSIONS

Micro-tsunami generated by the 28 January, 2000 earthquake (M_w = 6.8) occurred in the Southern Kuril subduction zone and was detected with high-precision ocean-bottom pressure gauges located about 200 km from the epicenter of the earthquake. We performed numerical computation of the micro-tsunami by employing seismic fault parameters. As a result, the micro-tsunami observed by two ocean-bottom pressure gauges, PG1 and PG2, of JAMSTEC was successfully represented by the numerical computations.

Such micro-tsunami seems could not be detected by traditional tide gauges along the coast. The high-precision measurements by offshore ocean-bottom pressure gauges, i.e. the vicinity of earthquake epicenters, have proved to have significant advantage of investigation of unsolved geophysical phenomena in the tsunami source areas.

REFERENCES

Hirata K., Aoyagi M., Mikada H., Kawaguchi K., Kaiho Y., Iwase R., Morita S., Fujisawa I., Sugioka H., Mitsuzawa K., Suyehiro K., Kinoshita H., and Fujiwara N., 2002: Real-time geophysical measurements on the deep seafloor using submarine cable in the southern Kurile subduction zone. *IEEE Ocean. Eng.*, **27** (2), 170-181.

Ohmachi T., Tsukiyama H., and Matsumoto H., 2001: Simulation of tsunami induced by dynamic displacement of seabed due to seismic faulting. *Bull. Seism. Soc. Am.,* **91** (6)**,** 1898-1909.

Takahashi H., and Hirata K., 2002: The 2000 Nemuro-Hanto-Oki Earthquake, off eastern Hokkaido, Japan – a key to solve the fault plane problem of the 1994 Kuril Earthquake (M_w = 8.3), submitted to *J. Geophys. Res.*